Roughness correction in the Casimir effect with metallic plates

2006 J. Phys. A: Math. Gen. 39 6517

(http://iopscience.iop.org/0305-4470/39/21/S49)

INSTITUTE OF PHYSICS PUBLISHING JOURNAL OF PHYSICS A: MATHEMATICAL AND GENERAL

J. Phys. A: Math. Gen. **39** (2006) 6517–6523 doi:10.1088/0305-4470/39/21/S49

Roughness correction in the Casimir effect with metallic plates

P A Maia Neto[1], Astrid Lambrecht[2] and Serge Reynaud[2]

[1] Instituto de Física, UFRJ, Caixa Postal 68528, Rio de Janeiro 21945-970, RJ, Brazil
[2] Laboratoire Kastler Brossel, CNRS, ENS, UPMC case 74, Campus Jussieu, 75252 Paris, France

Received 7 November 2005, in final form 23 December 2005
Published 10 May 2006
Online at stacks.iop.org/JPhysA/39/6517

Abstract

We compute the second-order roughness correction to the Casimir energy for two parallel metallic plates. We compare the proximity force and scattering approaches, showing that the former is obtained analytically in the limit of very smooth surfaces by neglecting non-specular reflections. We calculate the discrepancy between the two approaches for some typical numerical examples.

PACS numbers: 42.50.−p, 03.70.+k, 68.35.Ct

1. Introduction

The Casimir force between metallic plates has been measured with increasing experimental precision over the last 10 years [1]. Besides the intrinsic relevance of the Casimir effect, one important motivation is the search for non-Newtonian forces on the scale of a few hundred nanometres. The Casimir effect provides the dominant contribution to the force between metallic plates for separation distances in this range. Thus, in order to derive bounds for non-Newtonian forces from the experimental values, it is essential to compare them with an accurate theoretical model for the Casimir effect, taking into account all possible corrections to the ideal model considered by Casimir [2].

Two effects provide the dominant correction at separation distances of a few hundred nanometres: the finite conductivity of the metallic plates and the roughness of their surfaces. These two effects are not independent, and it would be pointless to calculate them separately and multiply the corresponding corrections. Moreover, the finite conductivity effect is not a small perturbation on the scale of a few hundred nanometres. Therefore, the roughness effect must be computed within a full finite-conductivity model for the metallic medium. We have recently presented the results of such a calculation [3, 4], taking the plasma model to describe the optical properties of the plates and considering the roughness effect to be a small perturbation.

In this paper, we discuss the physical meaning of the results for the roughness correction in different situations. We start by considering the approach based on the proximity force

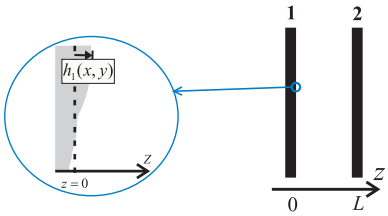

Figure 1. Parallel plates and detail of the internal surface of plate 1.

approximation (PFA). Then, we show how a more general result can be derived with the help of the scattering approach, in which the metallic plates are described by transfer operators. The resulting expression for the second-order correction is explained in terms of closed-loop diagrams involving non-specular reflections and polarization mixing. Finally, we present a second derivation of the PFA result, this time as a limiting case of the correction obtained in the scattering approach. This derivation explicitly shows that the PFA is equivalent, in the context of roughness, to neglecting the contribution of non-specular reflections.

2. Model

We consider two parallel rough metallic plates perpendicular to the z-axis, as shown in figure 1. The inner surface of plate j, with $j = 1, 2$ denoting each plate, is described by the profile function $h_j(\mathbf{r})$, where $\mathbf{r} = (x, y)$ collects the transverse coordinates. These functions define the local heights with respect to reference planes at $z = 0$ and $z = L$ and have zero spatial averages: $\langle h_j(\mathbf{r})\rangle = 0$. Hence, L represents the average separation distance. Both h_1 and h_2 are counted as positive when they correspond to local length decreases below the average L (as shown in figure 1, h_1 is positive along the positive z-axis, whereas h_2 is positive in the opposite direction). The profile functions are not prescribed or known experimentally; only some statistical information is available. The typical length scale for the variations of h_1 and h_2 along the xy-plane is the correlation length ℓ_C.

We make the following assumptions:

- The amplitude of roughness is very small compared to the average separation L:
$$|h_j(\mathbf{r})| \ll L, \qquad j = 1, 2. \tag{1}$$
This is the case in most Casimir experiments, where the amplitude is in the nanometre range, whereas L is of the order of a hundred nanometres or above.
- The slope of the surface profile is small:
$$|\nabla h_j(\mathbf{r})| \ll 1, \qquad j = 1, 2. \tag{2}$$
In terms of the correlation length ℓ_C, this condition reads $|h_j(\mathbf{r})| \ll \ell_C$. Although ℓ_C is not actually known in the experiments (see the discussion in the last section), one usually surmises that it is of the order of a few hundred nanometres. Equations (1) and (2) jointly allow us to consider the roughness as a small perturbation. They imply that the roughness amplitude is the smallest length scale in the problem. Accordingly, we compute the energy correction up to second order in h_1 and h_2.
- The plates are large enough to contain many correlation areas: $A \gg \ell_C^2$, where A is the area of the plates. Thus, they contain many statistically independent realizations of roughness profiles, as if the entire statistical ensemble were included in a single plate. Thanks to this assumption, we may identify spatial and statistical averages.

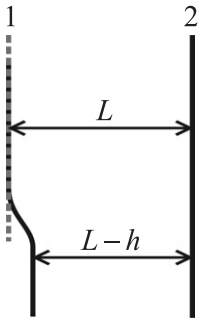

Figure 2. Roughness correction in the proximity force approximation.

- The two surfaces are statistically independent, so that the cross-correlation function vanishes:

$$\langle h_1(\mathbf{r})h_2(\mathbf{r}')\rangle = 0. \tag{3}$$

- Translational symmetry holds on the xy-plane. Hence, the self-correlation functions satisfy

$$\langle h_j(\mathbf{r})h_j(\mathbf{r}')\rangle = \langle h_j(\mathbf{r}-\mathbf{r}')h_j(\mathbf{0})\rangle, \qquad j = 1, 2. \tag{4}$$

From this condition, it follows that the Fourier transforms $H_j(\mathbf{k})$ ($\mathbf{k}$ is a two-dimensional vector) satisfy

$$\langle H_j(\mathbf{k})H_j(\mathbf{k}')\rangle = (2\pi)^2\delta^{(2)}(\mathbf{k}+\mathbf{k}')\sigma_j(\mathbf{k}), \qquad j = 1, 2, \tag{5}$$

where $\sigma_j(\mathbf{k})$, the roughness spectrum for plate j, is the Fourier transform of $\langle h_j(\mathbf{r})h_j(\mathbf{0})\rangle$.

3. Proximity force approximation

If, in addition to the assumptions listed above, we also assume that the correlation length ℓ_C is much larger than the mean separation distance L, then one may easily derive the roughness correction by taking the proximity force approximation [5].

With $L \ll \ell_C$, the surfaces are nearly flat over long distances (as compared to the separation). As a consequence, we may divide them into flat sections, with each section still much larger than L, as indicated in figure 2. The energy for each section is then given by the standard parallel-planes result for very large plates (since the slope of the surface profiles is very small). Although the Casimir energy is not additive, we may obtain an approximation for the total energy by adding the individual contributions of all sections:

$$E = \int e_{PP}\,(L - h_1(\mathbf{r}) - h_2(\mathbf{r}))\,\mathrm{d}x\,\mathrm{d}y, \tag{6}$$

where the integral is over the entire plate and $e_{PP}(z) = E_{PP}(z)/A$ is the Casimir energy per unit area for parallel planes separated by a distance z.

The interpretation of equation (6) goes as follows: the Casimir energy in the PFA is obtained from the parallel-planes result by simply averaging the *local* separation distance $L - h_1(\mathbf{r}) - h_2(\mathbf{r})$ over the surface of the plate.

Expanding the rhs of equation (6) in powers of h_j up to second order, we find

$$E = E_{PP}(L) - E'_{PP}(L)\langle h_1 + h_2\rangle + \frac{E''_{PP}(L)}{2}\langle (h_1 + h_2)^2\rangle, \tag{7}$$

where the primes denote derivatives. The first-order correction only depends on the global displacements of the plates and, thus, is a trivial effect (this is also the case for the more general theory discussed in the next section). Here it vanishes because of our definition for h_j. Hence, the roughness correction is of second order. Using equation (3), we find [6]

$$\delta E = E - E_{\rm PP} = \frac{E''_{\rm PP}(L)}{2}\langle h_1^2 + h_2^2\rangle, \tag{8}$$

Similar results, obtained from integration of the Casimir–Polder pairwise interaction, were used for comparison with experiments [7].

According to equation (8), the roughness correction derived from the PFA depends only on the *variance* of the surface profile. On the other hand, in the more general case discussed in the next section, with arbitrary values for $L/\ell_{\rm C}$, the correction depends on the *complete* roughness spectrum.

4. Scattering approach

In order to be more general, we follow the scattering approach [8] and consider the parallel plates as a plane cavity modifying the vacuum fluctuations in the intracavity region. The cavity is analysed as a composed optical network, where each component is described by a transfer operator [9]. This allows one to derive the intracavity field fluctuation from the free-space fluctuations propagating from outside.

Using this method, [9] obtained the following representation for the Casimir force in the ideal plane case:

$$F_{\rm PP} = -A\sum_p \int \frac{{\rm d}^2k}{(2\pi)^2}\int_0^\infty \frac{{\rm d}\omega}{2\pi}\hbar k_z(g_p(\mathbf{k},\omega) - 1), \tag{9}$$

where p denotes field polarization, $\mathbf{k}$ and $k_z = \sqrt{\omega^2/c^2 - k^2}$ are the wavevector components along the xy-plane and the z-axis, respectively, and $g_p(\mathbf{k},\omega)$ is the generalized Airy function for the plane cavity. The term $g_p(\mathbf{k},\omega) - 1$ in this equation quantifies the boundary effect of the cavity, modifying the vacuum fluctuations in the region between the plates. It is written in terms of the loop function $f_p(\mathbf{k},\omega)$ as follows (c.c. denoting the complex conjugate): $g_p(\mathbf{k},\omega) - 1 = f_p(\mathbf{k},\omega) + {\rm c.c.}$, with

$$f_p(\mathbf{k},\omega) = \frac{r_1(\mathbf{k},\omega)r_2(\mathbf{k},\omega)\,{\rm e}^{2{\rm i}k_zL}}{1 - r_1(\mathbf{k},\omega)r_2(\mathbf{k},\omega)\,{\rm e}^{2{\rm i}k_zL}}. \tag{10}$$

Thus, the generalized Airy function is determined by the reflection coefficients r_1 and r_2 of each plate (as seen from the intracavity region) and by the separation distance L.

We may write the loop function as the superposition of all propagation factors representing a closed loop, with an integer number of round trips inside the cavity:

$$f_p(\mathbf{k},\omega) = r_1(\mathbf{k},\omega)r_2(\mathbf{k},\omega)\,{\rm e}^{2{\rm i}k_zL} + \left[r_1(\mathbf{k},\omega)r_2(\mathbf{k},\omega)\,{\rm e}^{2{\rm i}k_zL}\right]^2 + \cdots. \tag{11}$$

The roughness correction of the Casimir force is similarly derived from the modification of the Airy function induced by the roughness effect:

$$\delta F = -A\sum_p \int \frac{{\rm d}^2k}{(2\pi)^2}\int_0^\infty \frac{{\rm d}\omega}{2\pi}\hbar k_z\delta g_p(\mathbf{k},\omega). \tag{12}$$

The second-order correction $\delta g_p(\mathbf{k},\omega)$ is written in terms of loop functions corresponding to round trips containing non-specular reflections:

$$\delta g_p(\mathbf{k},\omega) = \delta f_p^{(\rm i)}(\mathbf{k},\omega) + \delta f_p^{(\rm ii)}(\mathbf{k},\omega) + {\rm c.c.} \tag{13}$$

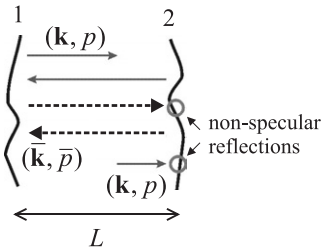

Figure 3. Diagram representing a second-order loop function.

The loop function $\delta f_p^{(\mathrm{i})}(\mathbf{k}, \omega)$ contains two first-order (non-specular) 'rough' reflections at the same plate (omitting the frequency dependence):

$$\delta f_p^{(\mathrm{i})}(\mathbf{k}) = \sum_{\bar{p}} \int \frac{\mathrm{d}^2\bar{k}}{(2\pi)^2} \big[r_{1;p}(\mathbf{k})\, \mathrm{e}^{2\mathrm{i}k_z L} R^{(1)}_{2;p\bar{p}}(\mathbf{k}, \bar{\mathbf{k}}) r_{1;\bar{p}}(\bar{\mathbf{k}})\, \mathrm{e}^{2\mathrm{i}\bar{k}_z L} R^{(1)}_{2;\bar{p}p}(\bar{\mathbf{k}}, \mathbf{k}) + \cdots \big] \sigma_2(\bar{\mathbf{k}} - \mathbf{k}) + [1 \leftrightarrow 2], \tag{14}$$

where $R^{(1)}_{2;\bar{p}p}(\bar{\mathbf{k}}, \mathbf{k}) H_2(\bar{\mathbf{k}} - \mathbf{k})$ is the first-order non-specular reflection coefficient changing the incident polarization p into $\bar{p}$ and the incident wavevector $\mathbf{k}$ into $\bar{\mathbf{k}}$. It is calculated by taking the Rayleigh hypothesis [10]. Whereas diffraction by the surface changes the value of $\mathbf{k}$, the frequency is conserved, since the surface is at rest. We have used equation (5) to write the average $\langle |H_j(\mathbf{k})|^2 \rangle$ in terms of the roughness spectrum $\sigma_j(\mathbf{k})$.

This expression should be read from right to left and corresponds to the diagram shown in figure 3. The first rough reflection at plate 2 changes $(\mathbf{k}, p)$ into $(\bar{\mathbf{k}}, \bar{p})$. This is followed by a round-trip propagation containing a specular reflection at plate 1 (factor $r_{1;\bar{p}}(\bar{\mathbf{k}})\, \mathrm{e}^{2\mathrm{i}\bar{k}_z L}$), and then by a second first-order non-specular reflection at plate 2, which changes polarization and momentum back to their original values. To close the loop, one must also return to the initial direction of propagation, by taking another 'specular' round trip. Additional diagrams are obtained by interposing arbitrary numbers of specular round trips between the stages described above. They are represented by the dots in equation (14), and can be added analytically as in equations (10) and (11).

Of course, we also add the diagrams corresponding to two non-specular reflections at plate 1 (the second line in equation (14)). Note, on the other hand, that diagrams with non-specular reflections at *different* plates do not contribute to the stochastic roughness correction when the surfaces are statistically independent because of equation (3).

As usual in second-order perturbation theory, we integrate over all intermediate modes of propagation to obtain the loop function $\delta f_p^{(\mathrm{i})}(\mathbf{k}, \omega)$ in equation (14).

The loop function $\delta f_p^{(\mathrm{ii})}(\mathbf{k}, \omega)$ can also be represented by diagrams like that discussed above. These diagrams contain a single *second-order* rough reflection at one of the plates.

If we assume that the two plates have the same optical properties, we may write the energy correction in terms of a single second-order roughness response function $G(k)$. By combining the previous equations and integrating δF over the separation distance, we find

$$\delta E = \int \frac{\mathrm{d}^2\mathbf{k}}{(2\pi)^2} G(k) \sigma(\mathbf{k}), \tag{15}$$

with $\sigma(\mathbf{k}) = \sigma_1(\mathbf{k}) + \sigma_2(\mathbf{k})$.

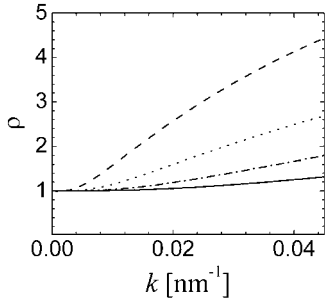

Figure 4. The sensitivity ρ as a function of k for the distances $L = 50$ nm (solid line), $L = 100$ nm (dashed-dotted line), $L = 200$ nm (dotted line) and $L = 400$ nm (dashed line).

Recovering PFA as a limiting case. If the roughness spectra are sharply peaked around $\mathbf{k} = \mathbf{0}$, we may approximate $G(k)$ by $G(0)$ in equation (15) and obtain

$$\delta E \approx G(0) \int \frac{\mathrm{d}^2\mathbf{k}}{(2\pi)^2} \sigma(\mathbf{k}) = G(0)\langle h_1^2 + h_2^2 \rangle, \tag{16}$$

in agreement with the PFA result, equation (8), provided that

$$G(0) = E''_{\mathrm{PP}}(L)/2. \tag{17}$$

The width of $\sigma(\mathbf{k})$ is of the order of the inverse correlation length $1/\ell_{\mathrm{C}}$, whereas the typical scale for the variation of $G(k)$ is of the order of $1/L$. Hence, the condition for the validity of the PFA is $L \ll \ell_{\mathrm{C}}$, in agreement with the discussion of the previous section.

It is instructive to analyse equation (14) in this limit. Since $\sigma_2(\bar{\mathbf{k}} - \mathbf{k})$ is peaked around $\mathbf{k} = \bar{\mathbf{k}}$, we may approximate $\bar{\mathbf{k}}$ by $\mathbf{k}$ in the coefficient $R^{(1)}_{2;\bar{p}p}(\bar{\mathbf{k}}, \mathbf{k})$. $R^{(1)}_{2;\bar{p}p}(\mathbf{k}, \mathbf{k})$ is the coefficient that describes *specular* reflection by a *plane* mirror which is displaced by a small quantity h_2. In this case, the correction simply amounts to introducing the phase shift $\mathrm{e}^{2\mathrm{i}k_z h_2}$ representing the additional round-trip propagation introduced by the displacement h_2, up to first order in h_2. Hence, it satisfies the condition $R^{(1)}_{2;\bar{p}p}(\mathbf{k}, \mathbf{k}) = 2\mathrm{i}k_z r_{2;p}(\mathbf{k})\delta_{\bar{p},p}$, regardless of the model considered for the material medium. Inserting this equation and the specular limits of the other coefficients into the expression for $G(k)$, we verify equation (17), showing that the PFA result can be derived from the general expression by discarding non-specular reflections at the plates. This is in line with the derivation of the previous section, where the surface was assumed to be nearly flat over long distances.

We may quantify the deviation from the PFA result by calculating the sensitivity function $\rho(k) = G(k)/G(0)$. We take the plasma model to describe the optical properties of the metallic plates, with a plasma wavelength $\lambda_{\mathrm{P}} = 136$ nm (corresponding to gold). In figure 4, we plot ρ as a function of k for different values of L. The value obtained in the scattering approach is always larger than the PFA result, and the discrepancy increases with the roughness wavevector k as expected, since larger values of k correspond to sharper variations of the surface profile. Clearly, the PFA is a better approximation for shorter distances, also as expected.

At $k = 0.02$ nm^{-1} (roughness wavelength $\sim$300 nm) and $L = 200$ nm, the correction is 60% larger than the PFA result.

5. Conclusion

We have analysed in detail the meaning of the PFA in the context of roughness, showing that it corresponds to the *specular limit* of the second-order correction obtained in the scattering

approach. So far, the roughness correction in recent experiments has been analysed only by a theoretical model equivalent to the PFA [7]. Thus, it is extremely important to investigate its accuracy given the real experimental conditions. A definite answer can only be reached by plugging the *complete* experimental roughness spectra $\sigma_j(\mathbf{k})$ into equation (15).

References

[1] Bordag M, Mohideen U and Mostepanenko V M 2001 *Phys. Rep.* **353** 1
Lambrecht A and Reynaud S 2002 *Sem. Poincaré* **1** 107
See also the present issue of *J. Phys. A: Math. Gen.* **39**
[2] Casimir H B G 1948 *Proc. K. Ned. Akad. Wet.* B **51** 793
[3] Maia Neto P A, Lambrecht A and Reynaud S 2005 *Europhys. Lett.* **69** 924
[4] Maia Neto P A, Lambrecht A and Reynaud S 2005 *Phys. Rev.* A **72** 012115
[5] Deriagin B V, Abrikosova I I and Lifshitz E M 1968 *Q. Rev.* **10** 295
Long J C, Chan H W and Price J C 1999 *Nucl. Phys.* B **539** 23
[6] Genet C, Lambrecht A, Maia Neto P and Reynaud S 2003 *Europhys. Lett.* **62** 484
[7] Klimchitskaya G L, Roy A, Mohideen U and Mostepanenko V M 1999 *Phys. Rev.* A **60** 3487
[8] Jaekel M T and Reynaud S 1991 *J. Physique* I **1** 1395 (*Preprint* quant-ph/0101067)
[9] Genet C, Lambrecht A and Reynaud S 2003 *Phys. Rev.* A **67** 043811
[10] Greffet J-J 1988 *Phys. Rev.* B **37** 6436